# Localized Biphasic Changes in Phosphatidylinositol-4,5-Bisphosphate at Sites of Phagocytosis

**Roberto J. Botelho,* Mary Teruel,¶ Renee Dierckman,‡ Richard Anderson,‡ Alan Wells,§ John D. York,‖ Tobias Meyer,¶ and Sergio Grinstein***

*Cell Biology Program, Hospital for Sick Children, and Department of Biochemistry, University of Toronto, Ontario M5G 1X8, Canada; ‡Department of Pharmacology, University of Wisconsin School of Medicine, Madison, Wisconsin 53706; §Department of Pathology, University of Pittsburgh, Pittsburgh, Pennsylvania 15261; ‖Department of Pharmacology and Cancer Biology and ¶Department of Cell Biology, Duke University Medical Center, Durham, North Carolina 27710

***Abstract.*** Phagocytosis requires localized and transient remodeling of actin filaments. Phosphoinositide signaling is believed to play an important role in cytoskeletal organization, but it is unclear whether lipids, which can diffuse along the membrane, can mediate the focal actin assembly required for phagocytosis. We used imaging of fluorescent chimeras of pleckstrin homology and C1 domains in live macrophages to monitor the distribution of phosphatidylinositol-4,5-bisphosphate (4,5-$PIP_2$) and diacylglycerol, respectively, during phagocytosis. Our results reveal a sequence of exquisitely localized, coordinated steps in phospholipid metabolism: a focal, rapid accumulation of 4,5-$PIP_2$ accompanied by recruitment of type Iα phosphatidylinositol phosphate kinase to the phagosomal cup, followed by disappearance of the phosphoinositide as the phagosome seals. Loss of 4,5-$PIP_2$ correlated with mobilization of phospholipase Cγ (PLCγ) and with the localized formation of diacylglycerol. The presence of 4,5-$PIP_2$ and active PLCγ at the phagosome was shown to be essential for effective particle ingestion. The temporal sequence of phosphoinositide metabolism suggests that accumulation of 4,5-$PIP_2$ is involved in the initial recruitment of actin to the phagocytic cup, while its degradation contributes to the subsequent cytoskeletal remodeling.

Key words: Fcγ receptors • phospholipase C • PH domain • diacylglycerol • phosphatidylinositol

## *Introduction*

Phagocytosis is an essential component of the innate immune response. During this process phagocytes internalize opsonized particles into a vacuole by an actin-dependent mechanism (Kwiatkowska and Sobota, 1999). Phagocytosis is triggered by the interaction of opsonins that coat the particle surface with receptors on the membrane of macrophages or neutrophils. These include the Fcγ receptors (FcγRs),[1] that bind specifically to the IgG found on antibody-coated particles (Daeron, 1997). After internalization, the phagosomal vacuole is converted into an effective microbicidal organelle by progressive fusion with endosomes and lysosomes (Beron et al., 1995).

Clustering of FcγRs on the surface of opsonized particles is associated with the phosphorylation of tyrosine residues within a defined region known as the immunoreceptor tyrosine-based activation motif (Greenberg et al., 1993, 1994). Src family kinases are thought to be responsible for phosphorylation of the immunoreceptor tyrosine-based activation motif, which bears two critically spaced tyrosines. Upon phosphorylation, the resulting phosphotyrosines serve as docking sites for the dual Src homology (SH2) domains of Syk (for review see Kwiatkowska and Sobota, 1999). Recruitment and activation of this tyrosine kinase is critical for FcγR-mediated phagocytosis, as demonstrated by the inability of macrophages from $Syk^{-/-}$ mice to internalize IgG-opsonized particles (Crowley et al., 1997; Kiefer et al., 1998). The downstream pathways stimulated by Syk are incompletely understood, but include phosphatidylinositol 3′-kinase (PI3K). This kinase appears to be essential for phagocytosis since inhibitors such as wortmannin impair particle engulfment (Ninomiya et al., 1994; Araki et al., 1996; Cox et al., 1999). Interest-

Address correspondence to Sergio Grinstein, Hospital for Sick Children, Division of Cell Biology, 555 University Ave., Toronto, Ontario M5G 1X8, Canada. Tel.: (416) 813-5727. Fax: (416) 813-5028. E-mail: sga@sickkids.on.ca

M. Teruel and T. Meyer's present address is Department of Molecular Pharmacology, Stanford University, Stanford, CA 94305-5174.

[1]*Abbreviations used in this paper:* CFP, cyan fluorescent protein; DAG, diacylglycerol; DIC, differential interference contrast; EGFP, enhanced GFP; ET-18-OCH3, 1-*O*-octadecyl-2-*O*-methyl-*sn*-glycerol-3-phosphorylcholine; FcγR, Fcγ receptor; $IP_3$, inositol-1,4,5-triphosphate; PH, pleckstrin homology; PI3K, phosphatidylinositol 3′-kinase; 4,5-$PIP_2$, phosphatidylinositol-4,5-bisphosphate; PIPKI, type I phosphatidylinositol phosphate kinase; PKC, protein kinase C; PLC, phospholipase C; SEM, scanning electron microscopy; SH, Src homology; TEM, transmission electron microscopy; TPA, 12-*O*-tetradecanoylphorbol-13-acetate; YFP, yellow fluorescent protein.

ingly, assembly of actin beneath the phagosomal cup persists in cells treated with wortmannin (Cox et al., 1999), suggesting that FcγRs can trigger actin polymerization by a pathway not involving PI3K.

Although crucial for particle internalization, the mechanism(s) underlying actin rearrangement are not well understood (Kwiatkowska and Sobota, 1999). Experiments using clostridial toxins or transfection of dominant-negative constructs have convincingly demonstrated that actin assembly during phagocytosis is mediated by Rho family GTPases (Cox et al., 1997; Hackam et al., 1997; Caron and Hall, 1998; Massol et al., 1998). At present, little is known about the downstream targets of these GTPases in phagocytosis. In other systems, however, Rho family GTPases were recently suggested (Chong et al., 1994; Tolias et al., 1995, 2000; Ren and Schwartz, 1998) to control actin polymerization by modulating the activity of type Iα phosphatidylinositol phosphate kinase (PIPKIα), which in turn controls the availability of phosphatidylinositol-4,5-bisphosphate (4,5-$PIP_2$). This phospholipid is thought to govern the distribution and function of a variety of cytoskeletal and signaling proteins that bear pleckstrin homology (PH) domains or lysine/arginine-rich hydrophobic motifs, which interact directly and specifically with the headgroup of 4,5-$PIP_2$ (Bottomley et al., 1998; Hinchliffe et al., 1998; Martin, 1998; Czech, 2000). It is not clear whether 4,5-$PIP_2$ functions similarly in phagocytosis.

In addition to its role as a direct docking site for skeletal proteins, 4,5-$PIP_2$ is also the primary substrate of phospholipase Cγ (PLCγ), which was shown to become activated upon engagement of FcγRs (Azzoni et al., 1992; Liao et al., 1992). The products of 4,5-$PIP_2$ hydrolysis, inositol-1,4,5-triphosphate ($IP_3$) and diacylglycerol (DAG), could in turn function as messengers in the cascade of events leading to phagocytosis. DAG and $IP_3$ could exert their effects by stimulating protein kinase C (PKC) isoforms and/or other DAG-binding proteins or by changing cytosolic calcium, respectively. However, the requirement for calcium and PKC in phagocytosis is controversial (Lew et al., 1985; Greenberg et al., 1991, 1993; Hishikawa et al., 1991; Zheleznyak and Brown, 1992).

It is apparent that the role of phosphoinositide metabolism in phagocytosis remains poorly defined. This paucity of knowledge can be attributed at least in part to the localized and transient nature of the phenomenon. These properties place constraints on the effectiveness of conventional biochemical analysis, since in a population of cells, receptor clustering and particle internalization occur asynchronously and only in a subdomain of the plasmalemma. These limitations can be overcome by direct analysis of single cells using spectroscopic methods. Recent and elegant reports have introduced the use of chimeric constructs of GFP with defined lipid-binding domains of proteins to monitor the distribution of phospholipids and their metabolites in transfected cells (Oancea and Meyer, 1998; Oancea et al., 1998; Stauffer et al., 1998; Varnai et al., 1999; Czech, 2000). In this report, we used fusion proteins of GFP or of its derivatives, yellow and cyan fluorescent proteins (YFP and CFP, respectively), with the PH domain of PLCδ or the C1 domain of PKCδ to monitor the dynamics of 4,5-$PIP_2$ and DAG, respectively, during phagocytosis. We present evidence for the occurrence of localized, biphasic changes in the concentration of 4,5-$PIP_2$ during phagocytosis. The mechanisms underlying these changes and their functional consequences were studied using pharmacological inhibitors and transfection of dominant-negative constructs.

## Materials and Methods

### Reagents and Antibodies

Dulbecco's minimal Eagle's medium, α-MEM, and fetal bovine serum were from Wisent Inc. U73122 and U73343 were from Biomol, Upjohn Laboratories, or Calbiochem. 1-*O*-octadecyl-2-*O*-methyl-*sn*-glycerol-3-phosphorylcholine (ET-18-OCH3) was from Biomol. Ionomycin and 1,2-dioctyl-*sn*-glycerol ($DiC_8$) were from Calbiochem. Hepes-buffered RPMI, human IgG, neomycin sulfate, 12-*O*-tetradecanoylphorbol-13-acetate (TPA), and wortmannin were from Sigma-Aldrich. Latex beads were from Bangs Laboratories. Rhodamine-phalloidin, Texas red–labeled zymosan, and Alexa 488–conjugated goat anti–rabbit were from Molecular Probes. Recombinant enhanced green fluorescent protein (EGFP) was from CLONTECH Laboratories, Inc. Sheep RBCs and rabbit anti–sheep RBC antibody were from ICN Biomedicals. Rabbit anti-PLCγ2 antibody was from Santa Cruz Biotechnology, Inc. Rabbit anti-PIPKIα antibodies were characterized previously (Zhang et al., 1997).

### DNA Constructs

The mammalian expression vectors pEGFP::AktPH, pEGFP::PLCδPH, pEGFP::PLCγSH2, and pEGFP::C1δ encode the PH domain of Akt (Kontos et al., 1998), the PH domain of PLCδ (Stauffer et al., 1998), the dual SH2 domains of PLCγ1 (Stauffer and Meyer, 1997), and the C1 domain of PKCδ, respectively, fused to EGFP. pCFP::PLCδ-PH and pYFP::C1δ encode the PH domain of PLCδ fused to CFP (PLCδ-PH-CFP) and the C1 domain of PKCδ fused to YFP (C1δ-YFP), respectively. pEGFP::PM-GFP encodes the 10–amino acid myristoylation/palmitoylation sequence from Lyn fused to EGFP (Teruel et al., 1999). pEGFP::PM-5′-phosphatase encodes a myristoylated/palmitoylated form of yeast INP54p, a 4,5-$PIP_2$–specific 5′-phosphatase, fused to EGFP (Raucher et al., 2000). pXf::PLCz encodes a dominant-negative fragment of PLCγ1 consisting of its SH2 and SH3 domains (Chen et al., 1996b).

### Cell Culture and Transfection

The macrophage RAW 264.7 cell line, obtained from the American Type Culture Collection, was maintained in Dulbecco's minimal Eagle's medium or α-MEM supplemented with 10% fetal bovine serum at 37°C, under a humidified 5% $CO_2$ atmosphere. Cells were transiently transfected with FuGENE 6 (Roche Molecular Biochemicals) according to the manufacturer's instructions and used within 24 h of transfection.

### Phagocytosis Assays

Sheep RBCs were opsonized with rabbit anti–sheep RBC antibody (1:50). Texas red–labeled zymosan and latex beads were opsonized with 1 mg/ml human IgG. Opsonization was for at least 1 h at room temperature, followed by three washes with PBS. To quantify phagocytosis, macrophages plated on coverslips were bathed in Hepes-buffered RPMI and overlaid with opsonized RBCs (≈50/macrophage). After incubating at 37°C for 15 min, RBCs that were not internalized were lysed by a brief exposure to water and the cells were fixed with 4% paraformaldehyde overnight at 4°C. The phagocytic index, defined as the number of phagosomes/100 macrophages, was estimated by differential interference contrast (DIC) microscopy. Where indicated, the onset of phagocytosis was synchronized by allowing the particles (≈20/cell) to bind to macrophages in ice-cold medium for 10 min, and ingestion was then initiated by addition of prewarmed medium.

### Immunofluorescence and Confocal Microscopy

To label F-actin, cells were fixed with paraformaldehyde, permeabilized in 0.1% Triton X-100, 100 mM glycine in PBS for 10 min and stained with a 1:400 dilution of rhodamine-phalloidin for 1 h. For immunofluorescence, cells were fixed and permeabilized as above and subsequently blocked with 5% donkey serum, followed by incubation with the primary antibodies for 1 h at room temperature. Rabbit anti-PLCγ2 and anti-PIPKIα were used at 1:50 and 1:100, respectively, in solutions containing 5% donkey serum. Finally, samples were incubated with Alexa 488–conjugated goat anti–rabbit antibody (1:1,000 dilution) for an additional 1 h.

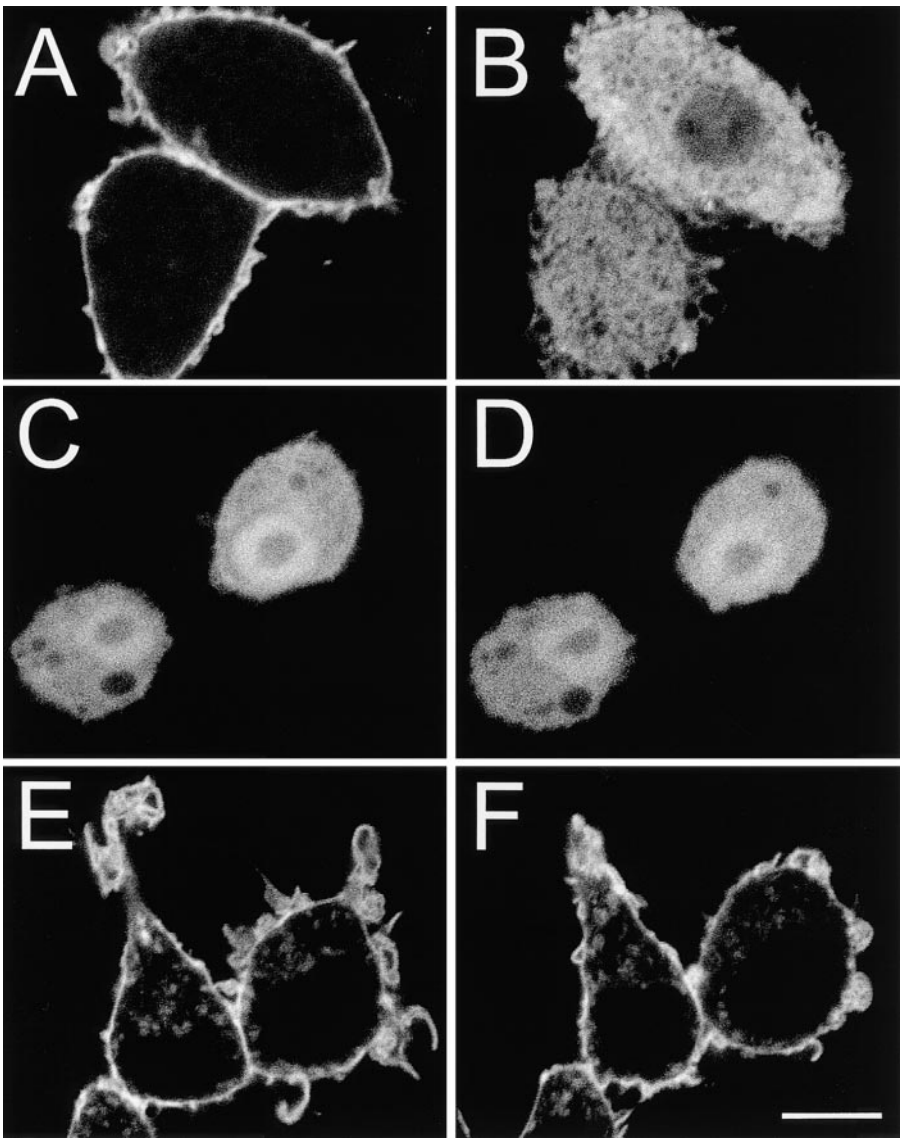


*Figure 1.* Distribution of PLCδ-PH-GFP, Akt-PH-GFP, and PM-GFP in RAW macrophages. RAW cells were transfected with PLCδ-PH-GFP (A and B), Akt-PH-GFP (C and D), and PM-GFP (E and F). Shown are representative cells before (A, C, and E) and after 10 min incubation in the presence of 10 μM ionomycin in medium containing 1.2 mM calcium (B, D, and F). Bar, 10 μm.

Both live as well as fixed and stained samples were analyzed by confocal microscopy using a LSM 510 laser scanning confocal microscope (ZEISS) with a 100× oil immersion objective. GFP/FITC and rhodamine/Cy3/Texas red were examined using the conventional standard laser excitation and filter sets. CFP and YFP constructs were sequentially excited by switching between the 458- and 514-nm laser lines, respectively. A band pass (BP480-520) emission filter was used for CFP whereas a long pass filter (LP560) was used for YFP.

Digital images were prepared using Adobe Photoshop® 4.0 (Adobe Systems Inc.) and CorelDraw® 8.0 (Corel Corp.). Quantitation of fluorescence was performed using NIH/Scion Image software.

### *Scanning and Transmission Electron Microscopy*

For transmission electron microscopy (TEM), cells were grown on 6-cm dishes. After induction of phagocytosis, the cells were rapidly washed with cold PBS, followed by a 2-h incubation in cold universal fixative (equal parts of 4% formaldehyde and 1% glutaraldehyde). The samples were then postfixed in 2% $OsO_4$ in 0.1 M phosphate buffer (pH 7.4). Dehydration was carried out in an ascending series of ethanol solutions. Subsequently the monolayer was embedded in Epon and cut into ultrathin sections, which were stained with uranyl acetate and lead citrate. Samples were examined and photographed in a Phillips EM 201C electron microscope.

For scanning electron microscopy (SEM), cells were grown on glass coverslips. Pseudopod extension was arrested by rinsing in ice-cold 0.1 M phosphate buffer (pH 7.4) before fixation as above. After several rinses in phosphate buffer, the cells were postfixed with buffered 1% $OsO_4$ for 1 h and dehydrated in ethanol. The samples were then critical point–dried and rendered conductive with a thin layer of gold. Samples were then examined and images acquired in a JEOL JSM 820 scanning electron microscope.

## *Results*

### *PLCδ-PH-GFP Is a Specific Probe for 4,5-$PIP_2$ in Macrophages*

The PH domain of PLCδ was shown to bind to 4,5-$PIP_2$ in vitro and in vivo with high affinity and specificity (Lemmon et al., 1995). Therefore, we used a fusion of this domain with GFP (PLCδ-PH-GFP) to analyze phospholipid metabolism in RAW 264.7 cells. As reported for other cell types (Stauffer et al., 1998; Varnai and Balla, 1998), PLCδ-PH-GFP associated predominantly with the plasmalemma of RAW cells, with little binding to organellar membranes (Fig. 1 A). Activation of endogenous PLC by elevation of cytosolic $Ca^{2+}$ using ionomycin caused extensive translocation of the chimera to the cytoplasm (Fig. 1 B), suggesting that PLCδ-PH-GFP is predominantly anchored to the plasma membrane through 4,5-$PIP_2$.

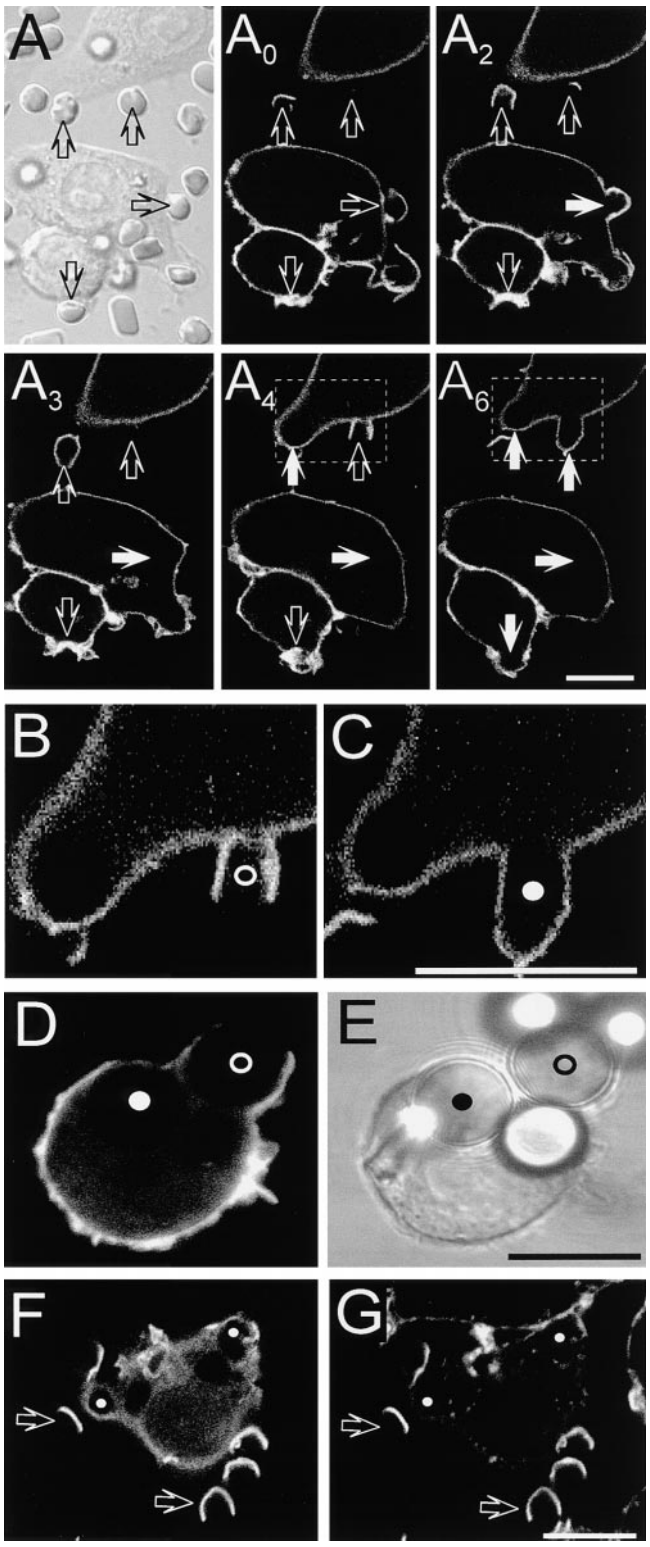


*Figure 2.* Distribution of PLCδ-PH-GFP during phagocytosis. Macrophages expressing PLCδ-PH-GFP were exposed to IgG-opsonized particles to induce phagocytosis. (A–C) Phagocytosis of RBCs. First panel is DIC image corresponding to the fluorescence image at $t = 0$ min. Subscripts (e.g., $A_0$) refer to the time in minutes at which the fluorescence images were captured. The times refer to the onset of recording, not to the time of addition of RBCs. Open arrows point to nascent phagosomes and solid white arrows show formed phagosomes. B and C are enlargements of the areas identified by boxes in $A_4$ and $A_6$. (D) Phagocytosis of 8-μm latex beads. (E) Corresponding DIC image. Nascent and formed phagosomes are indicated by open and filled circles, respectively, in B–E. (F and G) Macrophages expressing PLCδ-PH-GFP (F) were allowed to initiate phagocytosis of RBCs, followed by fixation and staining for F-actin with rhodamine-phalloidin (G). Open arrows point to phagocytic cups while the small filled white circles indicate formed phagosomes. Bars, 10 μm.

In vitro, the PH domain of PLCδ can also bind to phosphatidylinositol-3,4-bisphosphate (3,4-$PIP_2$) and phosphatidylinositol-3,4,5-trisphosphate (3,4,5-$PIP_3$), though with comparatively low affinity (Kavran et al., 1998). To assess the relative abundance of these lipids, RAW macrophages were transfected with the GFP-tagged PH domains of either Akt (Fig. 1, C and D) or Btk (not illustrated), which recognize specifically 3,4-$PIP_2$ and 3,4,5-$PIP_3$ (Kavran et al., 1998; Varnai et al., 1999). As depicted for Akt-PH-GFP, these fusion proteins were almost entirely in the cytosol before and after treatment with ionomycin (Fig. 1, C and D), implying that 3′-phosphorylated inositides are not abundant in unstimulated macrophages and that their contribution to the distribution of PLCδ-PH-GFP is likely negligible.

We also transfected RAW macrophages with PM-GFP, a myristoylated/palmitoylated GFP (Teruel et al., 1999). PM-GFP was preferentially targeted to the plasma membrane, although internal structures were also decorated (Fig. 1 E). Importantly, the distribution of PM-GFP was unaltered upon addition of ionomycin (Fig. 1 F), indicating that activation of PLC did not induce wholesale redistribution of the plasmalemmal lipids.

### *Redistribution of PLCδ-PH-GFP during Phagocytosis*

To monitor the distribution of 4,5-$PIP_2$ during phagocytosis, RAW cells transfected with PLCδ-PH-GFP were allowed to bind IgG-opsonized RBCs and fluorescence was measured in real time by confocal microscopy. Soon after addition of the opsonized particles, pseudopods labeled with PLCδ-PH-GFP extended from the macrophage surface and made contact with the RBCs (Fig. 2 A, open arrows). A biphasic change in fluorescence intensity was observed in the area of the membrane involved in phagocytosis. During pseudopod extension PLCδ-PH-GFP appeared to accumulate in phagocytic cups compared with the rest of the plasmalemma (Fig. 2 A, see also Fig. 4). This is best illustrated in panel $A_2$ of Fig. 2, where the downward-pointing open arrow denotes an area that is clearly more intense than the rest of the plasma membrane and where particle engulfment is about to occur (see 3–6-min sequence). In sharp contrast, once the phagocytic vacuole sealed, PLCδ-PH-GFP was no longer associated with the phagosomal membrane (Fig. 2 A, solid arrows). This is most clearly appreciated in the region of the phagosomal membrane most distant from the plasmalemma (i.e., the "base" of the phagosome), where differentiation of the two membranes is unambiguous. The distinction between surface and phagosomal membrane is clearly illustrated in Fig. 2, B and C, which are enlargements of the inset areas in the 4- and 6-min acquisitions of the top panel.

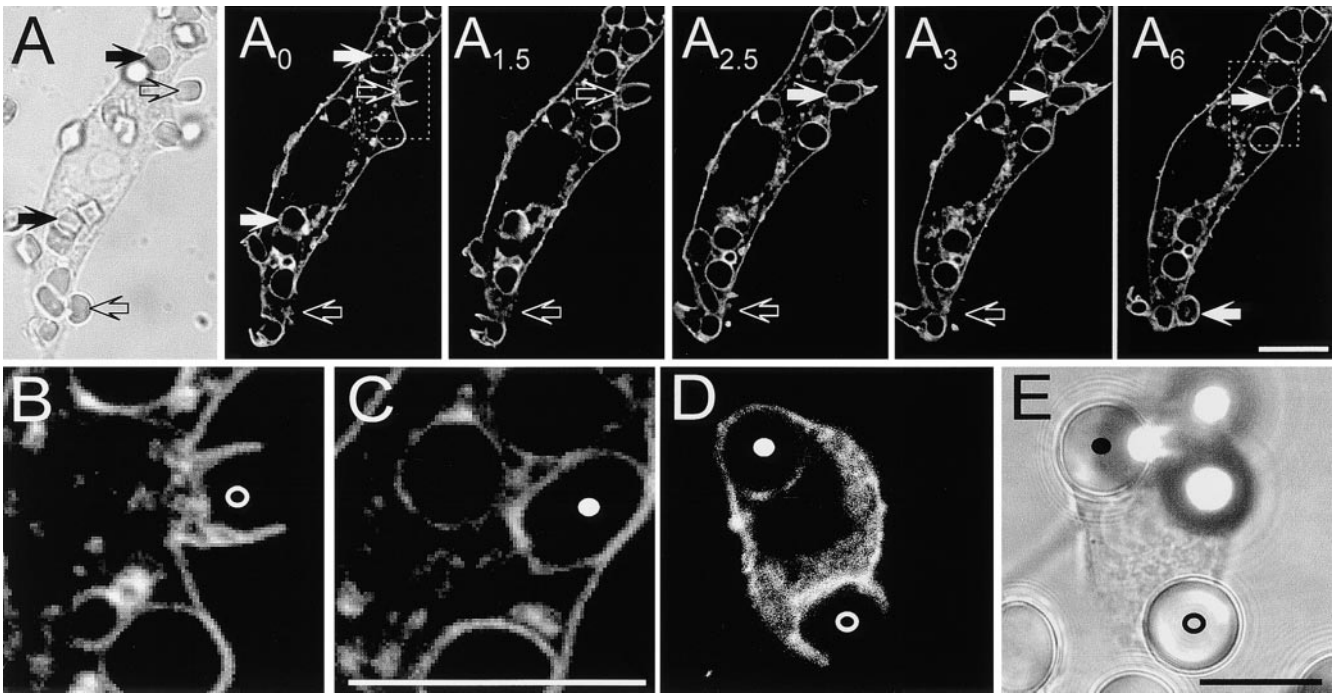


*Figure 3.* Phagocytosis in macrophages expressing PM-GFP. (A) DIC image and time course of phagocytosis, as described in the legend to Fig. 2 A. (B and C) Enlargements of the areas identified by boxes in $A_0$ and $A_6$. (D) Phagocytosis of 8-μm latex beads. (E) Corresponding DIC image. Bars, 10 μm.

The precise onset of the disappearance of 4,5-$PIP_2$ from the phagosomal membrane was difficult to assess using RBCs, since the time required for completion of phagocytosis and the distance between the PLCδ-PH-GFP–rich pseudopods and the base of the phagosome were short (e.g., open circle in Fig. 2 B). Therefore, we used larger particles (8-μm latex beads, IgG-opsonized) to define whether the second phase of 4,5-$PIP_2$ metabolism commences before or only after phagosomal sealing is complete. As in the case of opsonized RBCs, the larger beads were effectively internalized by RAW cells and, as before, fully formed phagosomes were devoid of PLCδ-PH-GFP (Fig. 2, D and E, filled circle). In addition, the larger size of the beads facilitated the detection of intermediate stages of phagosome formation and it was often possible to find phagosomal cups where the base of the phagosome was devoid of PLCδ-PH-GFP, whereas the fluorescent chimera was clearly detectable in the pseudopods (Fig. 2, D and E, open circle). This suggests that the onset of 4,5-$PIP_2$ conversion preceded phagosomal sealing.

The biphasic behavior of PLCδ-PH-GFP during phagocytosis closely resembled that of F-actin, which was revealed by staining with rhodamine-phalloidin. As reported previously, F-actin accumulated transiently underneath the phagosomal cup, where it is thought to propel the extension of pseudopods (Greenberg et al., 1991). As shown in Fig. 2, F and G (open arrows), sites of F-actin accumulation coincided with those regions where PLCδ-PH-GFP fluorescence was most intense. Upon particle internalization, F-actin was rapidly lost from the sealed phagosomes (indicated by filled circles in Fig. 2 G). The dissociation of actin paralleled the virtual loss of PLCδ-PH-GFP from the phagosomes (Fig. 2 F), signaling depletion of 4,5-$PIP_2$. These observations are consistent with a role of 4,5-$PIP_2$ in controlling actin remodeling during phagocytosis.

### *Distribution of PM-GFP during Phagocytosis*

The phagosomal membrane is known to undergo an active maturation process that involves progressive budding and concomitant fusion with endosomes and lysosomes (Beron et al., 1995). It is therefore conceivable that the observed loss of fluorescence from the early phagosomes could result from rapid replacement with endomembranes, which are ostensibly devoid of PLCδ-PH-GFP. This possibility was examined using PM-GFP, an acylated form of GFP that partitions preferentially to the inner monolayer of the plasma membrane (Teruel et al., 1999). Typical results are illustrated in Fig. 3 A. As expected, pseudopods labeled with PM-GFP were observed extending over RBCs (open arrows). However, in contrast to PLCδ-PH-GFP, the association of PM-GFP with the phagosomal membrane was persistent (Fig. 3 A, solid arrows). These observations are clearly illustrated in Fig. 3, B and C, which are magnified images of the enclosed areas in Fig. 3, $A_0$ and $A_6$. In fact, PM-GFP remained bound with phagosomes for at least 20 min after formation (not illustrated). Because RAW cells internalize multiple opsonized particles, this resulted in the progressive intracellular accumulation of brightly labeled phagosomes (Fig. 3 $A_6$).

The persistence of PM-GFP on the phagosome was also evident when using 8-μm latex beads. In this system, fluorescence was seen to surround the phagosome throughout the sealing process and to remain therein long after (Fig. 3, D and E, open and filled circles, respectively). These data indicate that rapid membrane turnover is not a likely explanation for the loss of PLCδ-PH-GFP from nascent pha-

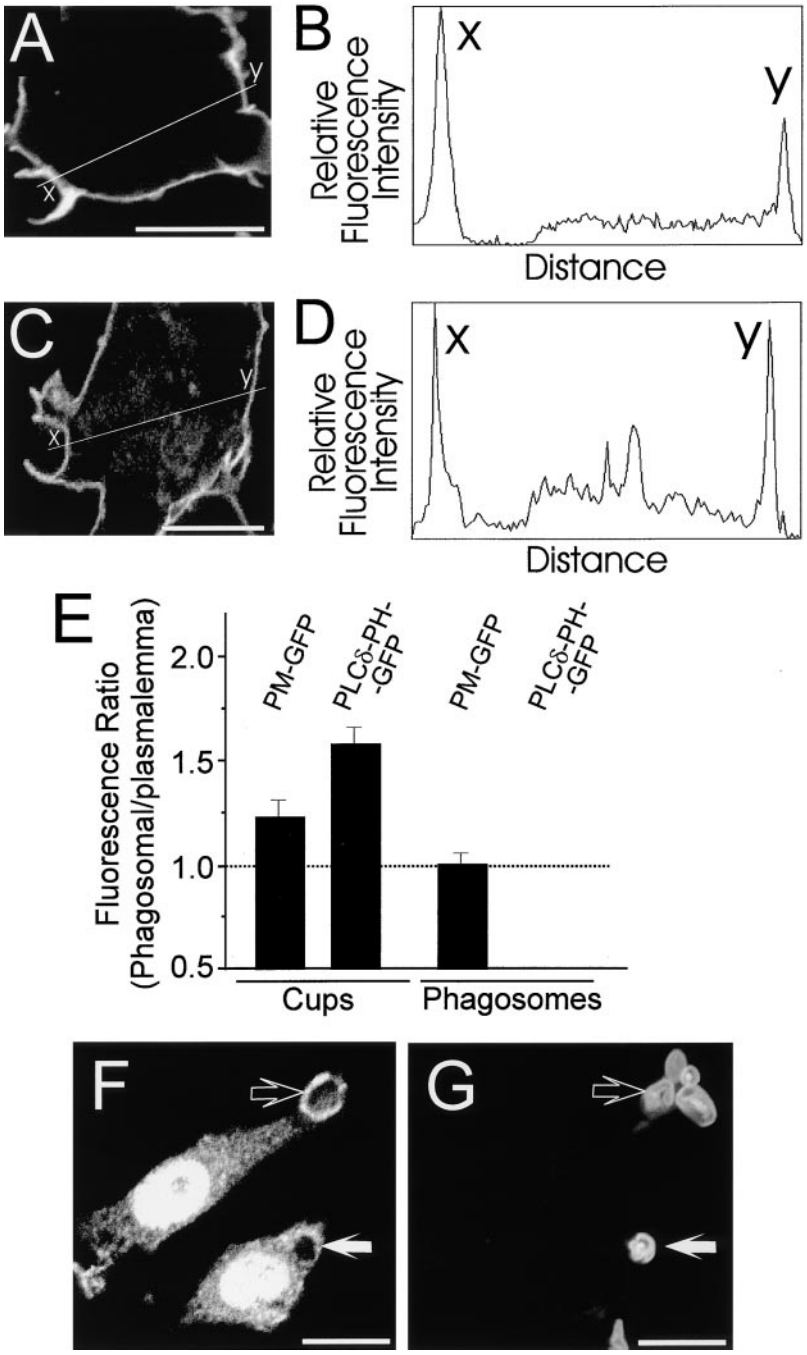


*Figure 4.* Quantification of phagosomal fluorescence. Confocal images of RAW cells undertaking phagocytosis were acquired as in the legends to Figs. 2 and 3. The digitized fluorescence intensity was quantified along line scans traversing both a phagosomal cup (x) and the contralateral plasma membrane (y). Representative images and corresponding quantitations are illustrated. (A and B) Cell transfected with PLCδ-PH-GFP. (C and D) Cell transfected with PM-GFP. (E) Ratio of the fluorescence at the phagosomal cup to the plasmalemma (two leftmost bars) or of the membrane of sealed phagosomes to the plasmalemma (two rightmost bars). The PLCδ-PH-GFP fluorescence of sealed phagosomes was negligible, yielding a ratio of ≈0. Means ± SE of 35, 64, 63, and 14 determinations, from left to right. (F) Distribution of PIPKIα during phagocytosis of Texas red–labeled zymosan particles (shown in G). Open arrow, nascent phagosome. Solid arrow, sealed phagosome. Bars, 10 μm.

gosomes. Rather, the loss of PLCδ-PH-GFP is occurring due to local changes in the availability of 4,5-$PIP_2$. This may result from sequestration, removal, or enzymatic conversion of the phosphoinositide during FcγR-mediated phagocytosis.

### *Accumulation of PLCδ-PH-GFP in Nascent Phagosomes*

To support our visual impression that PLCδ-PH-GFP, but not PM-GFP, was preferentially accumulated in phagosomal cups we quantified multiple digital images of early stages of phagocytosis. Line scanning of the base of the phagosome and of a contralateral area of the plasma membrane devoid of ruffles was performed as illustrated in Fig. 4, A–D, and the results of multiple determinations are summarized in Fig. 4 E. In the phagosomal membrane PLCδ-PH-GFP had peak intensities ranging from 1.3 to 2.3 times that of the plasma membrane (Fig. 4, A and B). The average ratio was 1.61 ± 0.08 (mean ± SE; $n = 64$, Fig. 4 E). In contrast, phagocytic cups labeled with PM-GFP had peak intensities ranging from 0.9 to 1.6 times that of the plasma membrane (Fig. 4, C and D). The average ratio in this case was 1.25 ± 0.08 ($n = 35$, Fig. 4 E), which is significantly different from unity ($t$ test, $P \leq 0.005$). This moderate, yet significant increase may reflect partition of PM-GFP into lipid rafts (Cheng et al., 1999) that may in turn accumulate in the phagosome. Regardless of the mechanism of accumulation of PM-GFP, a different process must underlie at least part of the accumulation of PLCδ-PH-GFP, which was significantly greater ($P < 0.005$). Increased net biosynthesis or preferential unmasking of 4,5-$PIP_2$ are likely possibilities.

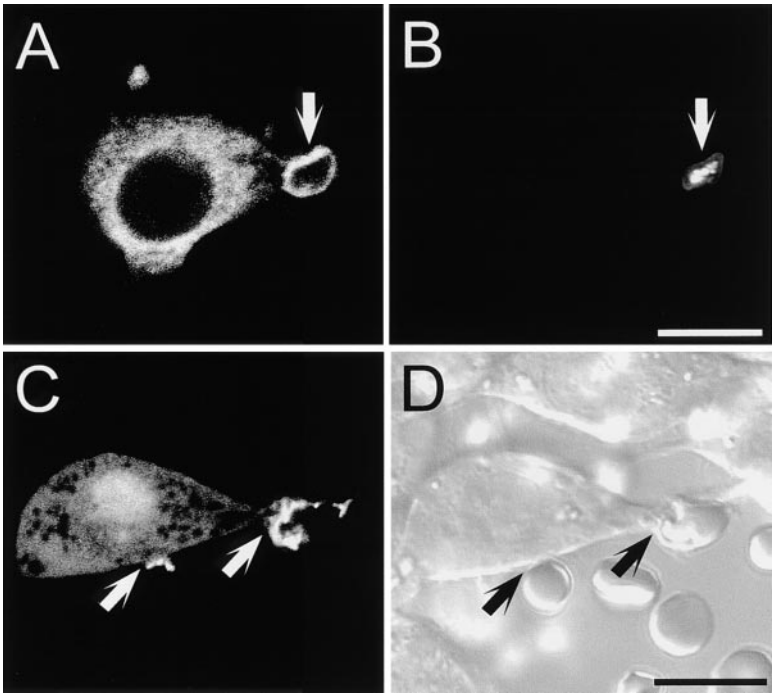


*Figure 5.* Distribution of PLCγ during phagocytosis. (A) Distribution of PLCγ2 during phagocytosis of Texas red–labeled zymosan particles (shown in B). (C) Distribution of PLCγ1-SH2-GFP during phagocytosis of RBCs (shown in D). Arrows in A–D point to nascent phagosomes. Bars, 10 μm.

We also quantified the amount of PM-GFP and PLCδ-PH-GFP in the formed (intracellular) phagosome. In this case, the density of phagosomal and plasmalemmal PM-GFP was virtually identical, whereas PLCδ-PH-GFP was essentially undetectable in the phagosome (Fig. 4 E). This quantitation confirms that bulk exchange of membrane during maturation is unlikely to account for the disappearance of PLCδ-PH-GFP from the sealed phagosome.

### *PIPKIα Concentrates in Phagocytic Cups*

The preferential accumulation of PLCδ-PH-GFP near the forming phagosome may reflect net formation of 4,5-$PIP_2$, as postulated for other processes where active actin remodeling occurs (Shibasaki et al., 1997; Martin, 1998; Tolias et al., 2000). To examine whether increased biosynthesis of the phosphoinositide occurs at the site of phagocytosis, we studied the distribution of PIPKIα isoforms by immunofluorescence. Although our antibodies were unable to detect PIPKIβ in RAW cells, positive immunoreactivity for PIPKIα was readily detected in these macrophages. Strikingly, upon addition of opsonized and fluorescently labeled particles, PIPKIα migrated to the nascent phagosome (Fig. 4, F and G, open arrow). The kinase dissociated from the phagosomal membrane shortly after completion of phagocytosis (Fig. 4, F and G, solid arrow). The transient association of PIPKIα with the nascent phagosome is consistent with the notion that 4,5-$PIP_2$ is locally accumulated during FcγR-mediated phagocytosis.

### *PLCγ Localizes to Phagocytic Cups*

Based on prior knowledge that PLCγ undergoes tyrosine phosphorylation during FcγR cross-linking (Azzoni et al., 1992; Liao et al., 1992), we hypothesized that the phase of dissociation of PLCδ-PH-GFP from phagosomes could be explained at least partly by PLC-mediated hydrolysis of 4,5-$PIP_2$. To validate this notion we studied the distribution of PLCγ2, the isoform expressed exclusively in hemopoietic cells, during the course of phagocytosis, using immunofluorescence. In unstimulated RAW macrophages, PLCγ2 was mostly cytosolic with slight accumulation in ruffling membranes (not illustrated). Significantly, we found that PLCγ2 accumulated intensely at sites of phagocytosis (Fig. 5, A and B). PLCγ is known to be recruited to the vicinity of activated receptors through interaction of its dual SH2 domains with phosphotyrosine residues on receptor–adaptor complexes (Rhee and Bae, 1997). A similar mechanism is likely involved during phagocytosis since, when transfected into RAW cells, the dual SH2 domains of PLCγ1 fused to GFP (PLCγ-SH2-GFP) were often seen to concentrate around phagocytic cups (Fig. 5, C and D).

### *Localized Generation of Diacylglycerol during Phagocytosis*

Activation of the PLCγ recruited to the phagocytic cup could account for the observed decrease in 4,5-$PIP_2$. To test this possibility, we examined the appearance of DAG using fusion proteins of the C1 domain of PKCδ with either GFP or YFP, hereafter named C1δ-GFP and C1δ-YFP, respectively. The C1 domain of PKCs was shown earlier to be an effective probe of DAG distribution in vivo (Oancea and Meyer, 1998; Oancea et al., 1998). Its use in RAW cells is illustrated in Fig. 6. In otherwise untreated cells, C1δ-GFP was exclusively associated with endomembranes, concentrating in a juxtanuclear complex (Fig. 6 A). Upon activation of endogenous PLC by calcium-ionomycin, a sizable fraction of C1δ-GFP translocated to the plasma membrane (Fig. 6 B). Likewise, treatment of the cells with TPA (Fig. 6 C) or $DiC_8$ (not shown) induced displacement of C1δ-GFP and C1δ-YFP to the plasmalemma. This implies that translocation of the C1δ fusion proteins during PLC activation occurs in response to the release of endogenous DAG and not to the concomitant increases in $IP_3$ and calcium concentration. Translocation of the C1δ chimeras to the plasma membrane persisted at 15°C (Fig. 6 C). This is consistent with the notion that the C1δ domain reaches the plasmalemma by diffu-

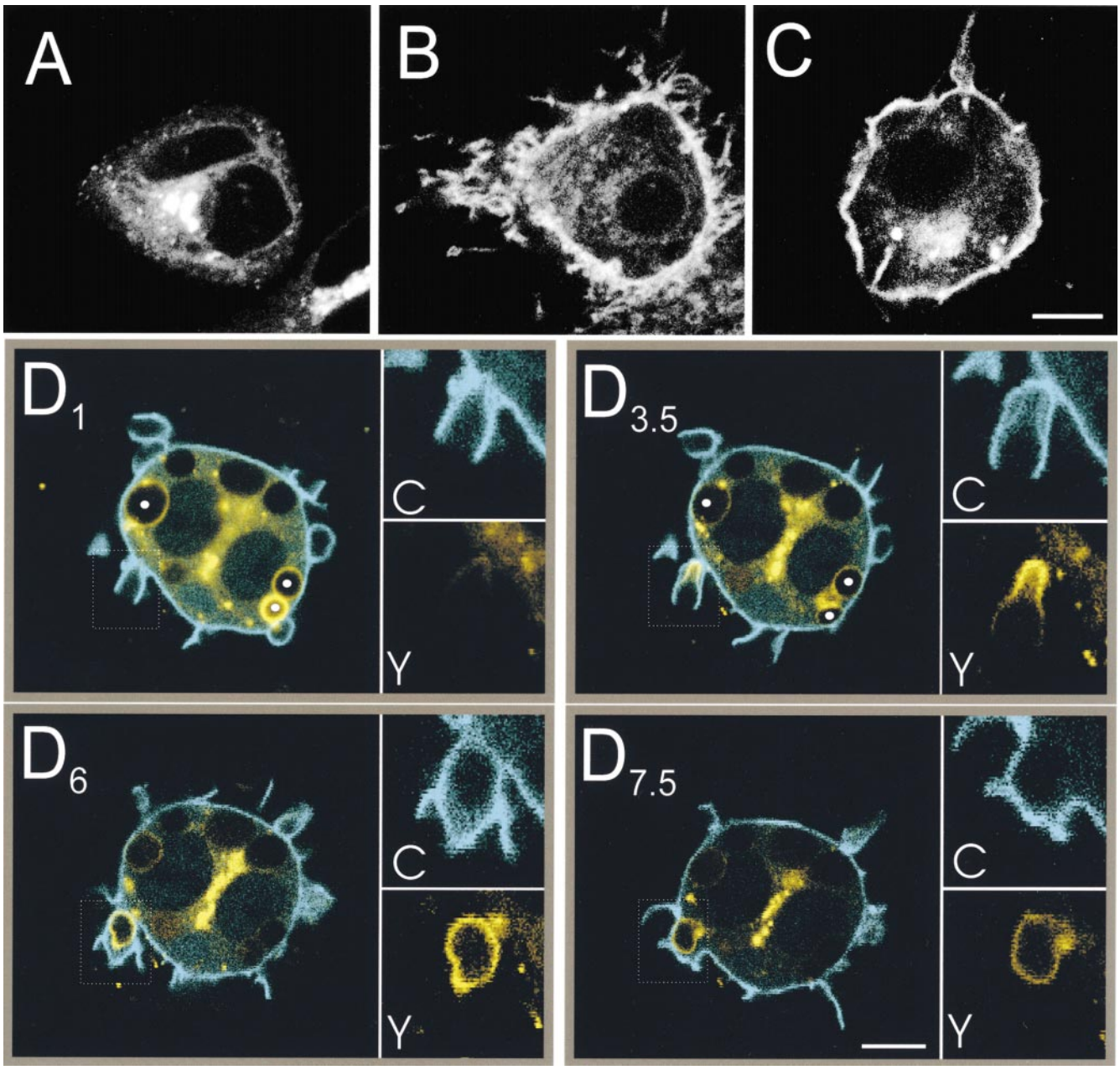


*Figure 6.* Distribution of C1δ-YFP and PLCδ-PH-CFP during phagocytosis. (A–C) Representative cells expressing C1δ-GFP or C1δ-YFP immediately before (A) and 10 min after addition of 10 μM ionomycin (B), or after treatment with 200 nM TPA for 10 min at 15°C (C). (D) Confocal fluorescence images of RAW cells coexpressing C1δ-YFP (yellow) and PLCδ-PH-CFP (blue) undergoing phagocytosis of RBCs. Subscripts (e.g., $D_1$) refer to the time in minutes at which the fluorescence images were captured. $D_1$, $D_{3.5}$, $D_6$, and $D_{7.5}$ show overlays of the PLCδ-PH-CFP and C1δ-YFP signals. The insets show separately the fluorescence of PLCδ-PH-CFP (labeled C) and C1δ-YFP (labeled Y) of the areas boxed by the dotted line. In $D_1$ and $D_{3.5}$, three formed phagosomes are indicated with filled white circles. Bars, 10 μm.

sion across the cytosol, after net dissociation from endomembrane binding sites. An alternative model, namely fusion of internal vesicles bearing C1δ domains with the plasma membrane, is unlikely due to the persistence of translocation at 15°C, since at this temperature vesicular traffic essentially ceases in mammalian cells. Moreover, we also observed modest yet reproducible accumulation of the C1 domain of PKCγ in forming phagosomes (not shown). In resting cells this domain is almost exclusively in the cytosol, ruling out translocation by vesicular fusion.

Having validated the sensitivity of these C1δ chimeras as indicators of DAG in RAW cells, we proceeded to study its distribution during phagocytosis. RAW macrophages were cotransfected with C1δ-YFP and PLCδ-PH-CFP, which enabled us to concomitantly examine the distributions of 4,5-$PIP_2$ and DAG in individual live cells by confocal microscopy. Fig. 6 D illustrates the course of redistribution of the two fluorophores after the addition of opsonized RBCs. C1δ-YFP was only weakly associated with the early phagocytic cup (Fig. 6 $D_1$, inset Y). At this stage, PLCδ-PH-CFP was enriched in the extending pseudopods (Fig. 6 $D_1$, inset C). As phagocytosis progressed, it was often possible to resolve the two membranes that constitute the phagocytic cup: the outside bi-

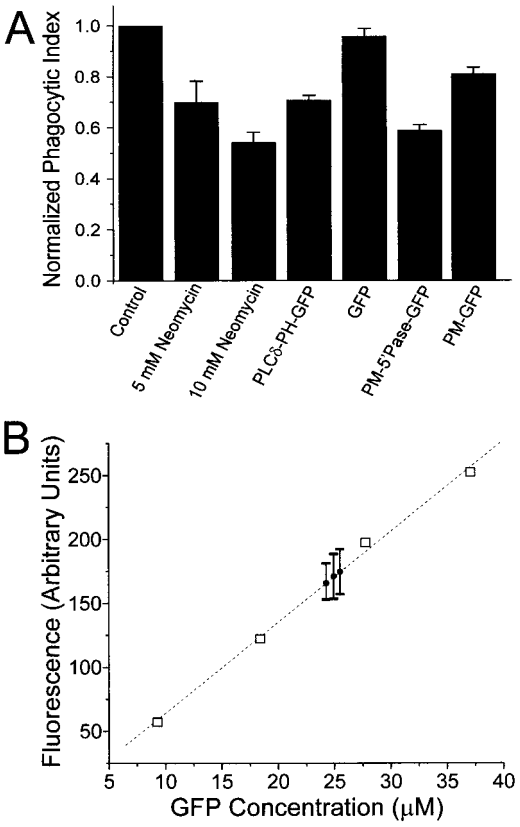


*Figure 7.* Sequestration and degradation of 4,5-$PIP_2$ attenuates phagocytosis. (A) Phagocytosis was quantified as described in Materials and Methods in RAW cells treated as follows (from left to right): control (untreated/untransfected); preincubated overnight with 5 or 10 mM neomycin sulfate; transfected with PLCδ-PH-GFP; transfected with GFP; transfected with PM-5′-phosphatase-GFP; transfected with PM-GFP. The phagocytic index was normalized to that of controls performed the same day. Data are means ± SE of 1,200 cells per condition. (B) Estimation of the concentration of PLCδ-PH-GFP expressed by RAW macrophages. To construct a calibration curve, droplets of solutions of recombinant EGFP at varying concentrations were placed under mineral oil and analyzed by confocal microscopy. The corresponding fluorescence is plotted versus EGFP concentration (squares). Cells transfected with PLCδ-PH-GFP were treated with ionomycin as in the legend to Fig. 1 and confocal images were acquired. Mean fluorescence of three experiments, each with ≥25 cells, is shown (circles with error bars representing SEM).

layer of the pseudopod remained labeled with PLCδ-PH-CFP throughout and eventually sealed to restore plasmalemmal continuity. In comparison, PLCδ-PH-CFP fluorescence diminished progressively in the inner bilayer of the pseudopods, i.e., the one more closely apposed to the particle and later becomes the phagosomal membrane (Fig. 6 $D_{3.5}$, inset C). The dissociation of PLCδ-PH-CFP from the inner bilayer was accompanied by recruitment of C1δ-YFP (Fig. 6 $D_{3.5}$, inset Y). Initially, this accumulation was most prominent at the base of the phagocytic cup, but it then extended toward the tips of the pseudopods before phagosome sealing. Importantly, C1δ-YFP labeling was usually strongest immediately after phagosome closure, at which time PLCδ-PH-CFP was completely absent from the phagosome (Fig. 6 $D_6$). The association of C1δ-YFP with the phagosome declined gradually thereafter (Fig. 6 $D_{7.5}$), becoming undetectable after several minutes. The full dissociation of C1δ-YFP from formed phagosomes can be clearly appreciated by inspecting the three sealed phagosomes indicated by filled circles in Fig. 6 $D_1$. Similar results were obtained with C1δ-GFP alone (not shown). These observations suggest that DAG is locally synthesized by PLC-mediated hydrolysis of 4,5-$PIP_2$ during phagosome formation and is subsequently converted in the sealed phagosome to other metabolites.

### *Reduced Availability of 4,5-$PIP_2$ Attenuates Fcγ R-mediated Phagocytosis*

The localized activation of 4,5-$PIP_2$ metabolism in the forming phagosome suggests a functional role for this phosphoinositide in phagocytosis. To verify this hypothesis, we tested the effects of several methods to reduce the availability of 4,5-$PIP_2$ on the ability of RAW cells to internalize opsonized particles. Neomycin sulfate is a somewhat permeant divalent cation that can compete with endogenous ligands for binding to 4,5-$PIP_2$. Overnight treatment with 5 and 10 mM neomycin reduced the phagocytic index by 30 ± 8 and 45 ± 5%, respectively ($n = 15$, $P < 0.001$; Fig. 7 A). Because neomycin may have nonspecific effects, we also tested other, more specific means of interfering with 4,5-$PIP_2$. PLCδ-PH-GFP can be used not only to monitor the distribution of 4,5-$PIP_2$, but when expressed at sufficiently high levels, also to competitively inhibit other 4,5-$PIP_2$–dependent processes. Accordingly, overexpression of this construct was shown recently to interfere with anchoring of the actin cytoskeleton to the plasma membrane (Varnai and Balla, 1998; Raucher et al., 2000). Effective scavenging of 4,5-$PIP_2$ by PLCδ-PH-GFP would only be expected to occur if the concentration of the latter can approximate or exceed that of its phosphoinositide ligand. Therefore, we estimated the intracellular concentration of PLCδ-PH-GFP in transfected RAW cells by comparison with microscopic droplets of standard solutions containing known concentrations of recombinant EGFP. As shown in Fig. 7 B, interpolation of the cell-associated fluorescence in such calibration curves yielded intracellular concentrations of ≈25 μM. This concentration should suffice to exert a significant scavenging effect on 4,5-$PIP_2$, which can be estimated to exist in the micromolar range, based on existing determinations of phospholipid content in several cell types.

Therefore, we proceeded to test the effects of PLCδ-PH-GFP expression on phagocytosis. In cells expressing PLCδ-PH-GFP the phagocytic index was reduced moderately (30 ± 2%; $n = 12$), yet significantly ($P < 0.0001$; Fig. 7 A). In contrast, the soluble, unmodified form of GFP had no significant effect on phagocytosis (Fig. 7 A).

We also attempted to decrease the availability of 4,5-$PIP_2$ by enzymatic means, expressing PM-5′-phosphatase-GFP in RAW macrophages. This chimeric protein consists of the yeast $INP54_p$, a 4,5-$PIP_2$–specific 5′-phosphatase, attached to the acylation sequence of Lyn to promote its association with the membrane, and to GFP to facilitate detection. This yeast phosphatase has been shown to reduce the content of 4,5-$PIP_2$ in COS cells (Raucher et al., 2000). The subcellular distribution of PM-5′-phosphatase-GFP was indistinguishable from PM-GFP when expressed in RAW macrophages but the cells had a tendency to round up (not illustrated). We found that expression of PM-5′-

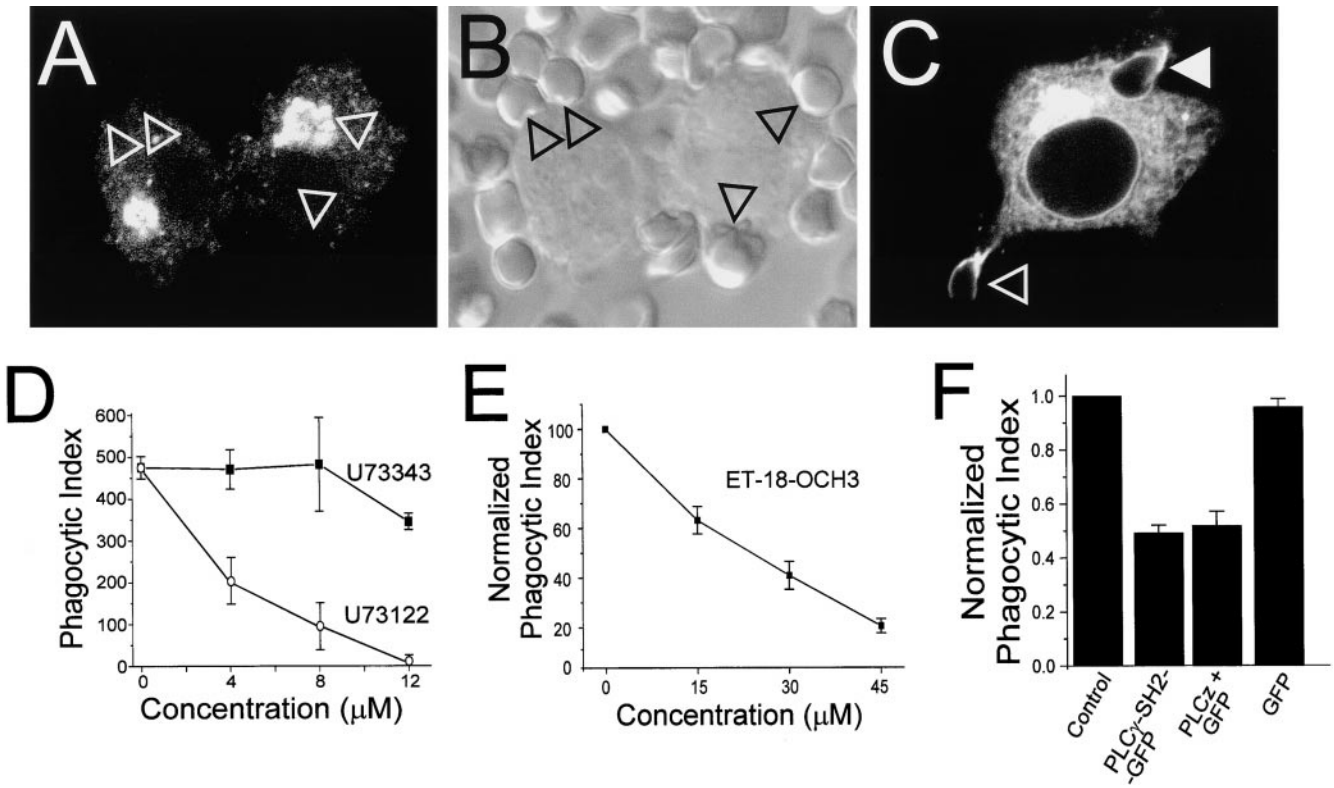


*Figure 8.* PLC is required for phagocytosis. (A–C) Macrophages expressing C1δ-GFP were pretreated with 6 μM U73122 (A) or U73343 (C) and subsequently allowed to interact with opsonized RBCs. B is a DIC image corresponding to A, showing adherent RBCs (arrowheads). In C, open arrowhead points to nascent phagosome, solid arrowhead to sealed phagosome. (D and E) RAW cells were pretreated for 15 min with the indicated concentrations of either U73343 (D, filled symbols), U73122 (D, open symbols), or ET-18-OCH3 (E) and phagocytosis was measured in the presence of the drugs. Data are means ± SE of three experiments (200 cells counted in each). (F) Phagocytosis was quantified in RAW cells treated as follows (from left to right): control (untransfected); transfected with the SH2 domains of PLCγ1; transfected with PLCz and GFP; transfected with GFP alone. The phagocytic index was normalized to that of controls performed the same day. Data are means ± SE of at least 1,200 cells per condition.

phosphatase-GFP reduced the phagocytic index of RAW macrophages by 42 ± 2% ($n = 12$, $P < 0.0001$; Fig. 7 A). This effect may not be entirely attributable to the phosphatase activity of the construct, since transfection with PM-GFP alone produced a modest, yet reproducible inhibition of phagocytosis (Fig. 7 A). It is conceivable that the acylated GFP displaces endogenous Src family kinases, which are also acylated and required for efficient phagocytosis. Jointly, these observations suggest that unhindered availability of 4,5-$PIP_2$ is required for optimal phagocytosis.

### *Inhibition of PLC Blocks Diacylglycerol Synthesis and Ablates Phagocytosis*

To test the role of PLC in phagocytosis, we used U73122 and ET-18-OCH3, two structurally different PLC-specific antagonists (Chen et al., 1996b). Inhibition of the phosphoinositide-specific PLC by U73122 was confirmed using the DAG-binding C1δ-GFP construct. Treatment with 6 μM U73122 for 15 min precluded accumulation of C1δ-GFP at the sites of RBC attachment (Fig. 8, A and B). In contrast, C1δ-GFP was recruited normally to the phagocytic cups in the presence of U73343, an inactive analogue of U73122, mirroring the effects of these agents on phagocytosis (Fig. 8 C). Importantly, U73122 did not block TPA-dependent recruitment of C1δ-GFP to the plasma membrane (not illustrated), indicating that U73122 does not directly bind to C1δ-GFP.

The dependence of FcγR-mediated phagocytosis on PLC was examined next. We found that U73122 inhibited phagocytosis in a dose-dependent fashion, with half-maximal effects at ≈3 μM (Fig. 8 D). In contrast, U73343 had no significant effect at up to 6 μM and had only a minor antagonistic effect at 12 μM (Fig. 8 D). Importantly, ET-18-OCH3, a structurally and mechanistically unrelated antagonist of PLC, also reduced phagocytosis in a dose-dependent fashion, with half-maximal inhibition at ≈25 μM (Fig. 8 E).

A more specific approach to inhibit PLCγ was also undertaken. Cells were transfected with two catalytically inactive fragments of PLCγ, namely PLCγ-SH2-GFP and PLCz, which were expected to exert a dominant-negative effect. PLCz contains the dual SH2 and SH3 domains of PLCγ1 and previously described PLC-inhibitory motif (Chen et al., 1996b). As illustrated in Fig. 8 F, macrophages transfected with PLCγ-SH2-GFP or PLCz had a markedly impaired ability to internalize opsonized RBCs. In both instances the phagocytic index dropped by >50% ($n = 12$; $P < 0.0001$). As before, paired experiments in which GFP alone was transfected showed no effect on phagocytosis. While we cannot rule out that PLCγ-SH2-GFP or PLCz bound to phosphotyrosine groups unrelated to those that anchor PLCγ, the unique sequence and spacing of these dual SH2 domains favor preferential association with the physiological target of the phospholipase. There-

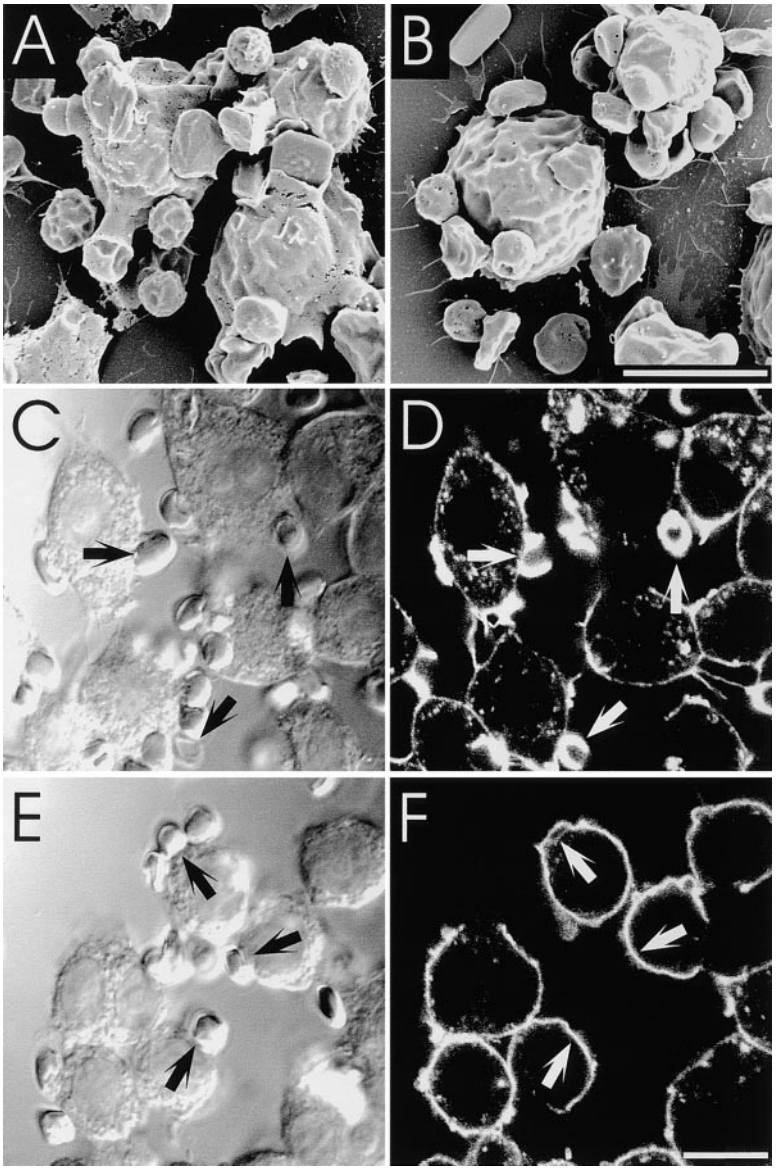


*Figure 9.* Effect of U73122 on pseudopod extension and actin cup formation. (A and B) RAW cells were treated without (A, C, and D) or with 5 μM U73122 (B, E, and F), allowed to bind RBCs on ice, and then warmed up for 4 min to initiate phagocytosis. The cells were then fixed and analyzed by SEM (A and B) or stained with rhodamine-phalloidin and analyzed by confocal microscopy (C–F). Arrows point to adherent RBCs. Bars, 10 μm.

fore, these findings suggest that PLCγ is an important regulator of FcγR-mediated phagocytosis.

### *Inactivation of PLC Abolishes Pseudopod and Actin Cup Formation*

To better define the stage of the phagocytic sequence requiring PLC, we examined whether pseudopod extension and actin polymerization occurred in cells treated with U73122 and ET-18-OCH3. Pseudopod morphology was evaluated by SEM and TEM. In control cells (either untreated or treated with the inactive analogue U73343), the formation of pedestals below the RBCs and the extension of pseudopods around them were readily observable (Fig. 9 A). In contrast, cells treated with U73122 were unable to extend pseudopods or form pedestals, even though RBCs appeared tightly attached to the surface of the macrophages (Fig. 9 B). This impression was verified using TEM. As before, in control cells pseudopods were observed elongating along the surface of RBCs (not illustrated). By comparison, the extension of pseudopods in U73122-treated cells was minimal.

Not only was pseudopod extension inhibited by U73122, but actin remodeling under the cup was similarly obliterated. Although in normal cells marked F-actin accumulation delineates the phagocytic cup (Fig. 9, C and D), as reported by others (Sheterline et al., 1984; Greenberg et al., 1991; Kwiatkowska and Sobota, 1999), virtually no accumulation was noted in cells treated with the PLC blocker, despite normal adherence of RBCs to their surface (Fig. 9, E and F). Similar results were obtained by treating cells with 80 μM ET-18-OCH3 in the presence of 10% serum (not depicted). These observations differ from those described in cells incubated with the PI3K inhibitor wortmannin. While wortmannin-treated cells fail to internalize particles, they nevertheless display marked actin reassembly under the adherent RBCs (Araki et al., 1996; Cox et al., 1999; and our own observations, not shown).

The inability of cells to form pseudopods and actin cups upon incubation with U73122 and ET-18-OCH3 is not the result of a detrimental effect of the drug on cellular viability. These effects were fully reversible. Moreover, in the presence of the drug, pinocytosis of FITC-dextran appeared to be unimpaired (data not shown). We conclude that inhi-

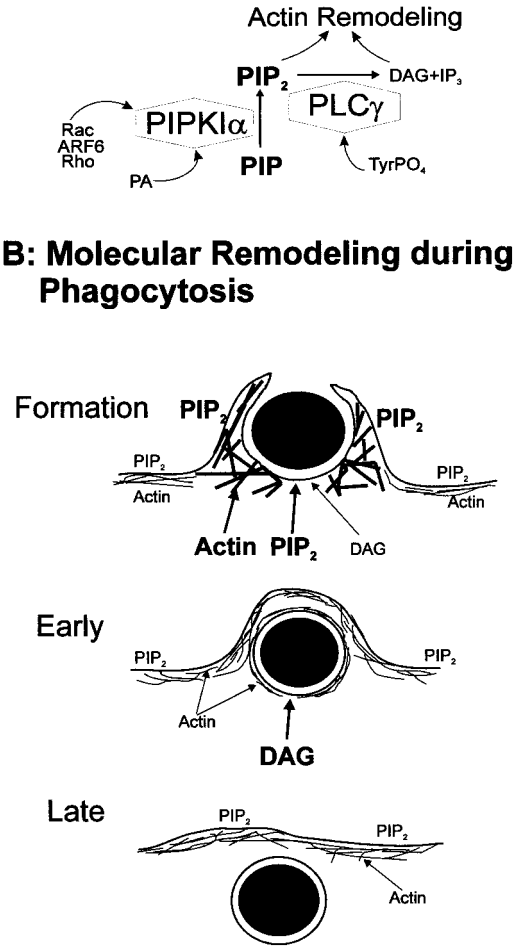


*Figure 10.* Lipid signaling and actin redistribution during phagocytosis. (A) Putative events mediating 4,5-$PIP_2$ metabolism at the nascent phagosome. (B) Diagrammatic representation of the sequence of events during phagosome formation and internalization. The font size is indicative of the relative abundance of the components (e.g., more 4,5-$PIP_2$ at the phagosomal cup than in the plasmalemma during formation). Note that: (a) actin and 4,5-$PIP_2$ are enriched in the phagosomal cup during formation; (b) DAG appears during formation, but is most abundant shortly after completion of phagocytosis (Early stage); (c) neither 4,5-$PIP_2$ nor DAG are detectable in "late" phagosomes (Late stage); (d) phagosomal actin decreases in parallel with or shortly after 4,5-$PIP_2$; (e) 4,5-$PIP_2$ is present at the nonphagosomal plasma membrane throughout the phagocytic process; and (f) we postulate that PLC activity is required to induce actin disassembly and remodeling during cup formation and phagosomal closure.

bition of PLC arrests phagocytosis at an early stage, and is required for actin remodeling during pseudopod formation.

## *Discussion*

### *Suitability of GFP Chimeras as Probes*

To monitor the distribution and metabolism of 4,5-$PIP_2$ and DAG during phagocytosis, we used chimeras consisting of GFP, or its derivatives, and the PH domain of PLCδ or the C1 domain of PKC, respectively. These probes had been validated in other systems (Oancea et al., 1998; Stauffer et al., 1998; Varnai and Balla, 1998) and their suitability was confirmed in RAW macrophages. In brief, PLCδ-PH-GFP localized almost exclusively to the plasmalemma of untreated cells, but redistributed to the cytosol when PLC was activated (Fig. 1, A and B). Moreover, though this chimera also has measurable affinity for 3′-phosphorylated inositides in vitro, the abundance of the latter in resting cells was found to be negligible compared with 4,5-$PIP_2$ (Fig. 1 C). The increase in 3,4,5-$PIP_3$ predicted to occur during phagocytosis, based on the reported activation of PI3K (Araki et al., 1996; Cox et al., 1999), did not affect the distribution of PLCδ-PH-GFP. Indeed, this construct detached from the phagosomal membrane as 3,4,5-$PIP_3$ accumulated, as revealed by the recruitment to the phagosome of chimeras of Akt or BTK-PH domains with GFP (our unpublished observations). Therefore, PLCδ-PH-GFP appears to be exquisitely selective for 4,5-$PIP_2$ in RAW cells.

C1δ-GFP seems similarly appropriate for the detection of DAG. It redistributed to the plasma membrane when endogenous PLC was activated with ionomycin, leading to production of DAG synthesis (Fig. 6, A and B), as well as upon addition of phorbol esters (Fig. 6 C) or exogenous DAG (not shown). Such translocation appears to occur by dissociation of the C1δ domain from its internal reservoir, followed by diffusion across the cytosol and association with plasmalemmal DAG. A possible alternative mode of translocation, namely fusion of endomembrane vesicles with the surface membrane, is unlikely based on the temperature insensitivity of the process and on the finding that C1γ-GFP, which is in the cytosol of unstimulated cells (Oancea et al., 1998; and our unpublished observations), also accumulated in the phagosomal cup.

### *Biphasic Changes in 4,5-$PIP_2$ during Phagocytosis*

Shortly after addition of the opsonized particles, PLCδ-PH-GFP was found to accumulate on the membrane of the developing phagosome. The accumulation of the 4,5-$PIP_2$ probe exceeded that of PM-GFP, implying that it is not simply due to folding of the membrane during pseudopod extension (Figs. 2–4). Instead, we attribute the concentration of PLCδ-PH-GFP in the phagocytic cups to increased local synthesis of 4,5-$PIP_2$. In support of this conclusion, we noticed local recruitment of PIPKIα to phagocytic cups (Fig. 4).

The initial accumulation of PLCδ-PH-GFP was transient and was followed immediately by its abrupt dissociation from formed phagosomes (Fig. 2, see also Fig. 6 D). This behavior contrasted strikingly with that of PM-GFP, which remained associated with phagosomes for the duration of our analysis (Fig. 3), ruling out rapid membrane turnover as the process responsible for the loss of PLCδ-PH-GFP. A priori, several potential mechanisms could explain the detachment of the PLCδ-PH probe. First, the probe may be displaced by a ligand(s) with higher affinity for 4,5-$PIP_2$. Second, lipid transferase proteins may selectively remove 4,5-$PIP_2$ from nascent and early phagosomes. Third, 4,5-$PIP_2$ could be enzymatically converted to products no longer recognized by fluorescent fusion proteins of PLCδ-PH. In this regard, there are at least three types of enzymatic activities that could contribute to

the disappearance of 4,5-$PIP_2$. Type II inositol polyphosphate phosphatases can convert 4,5-$PIP_2$ to its monophosphorylated precursors, which have poor affinity for PLCδ-PH-GFP. It is interesting to note that a type II phosphatase active towards 4,5-$PIP_2$ was found to localize to ruffling membranes (Mochizuki and Takenawa, 1999). A similar accumulation on the phagosomal membrane would contribute to 4,5-$PIP_2$ disappearance. Alternatively, 4,5-$PIP_2$ could be consumed by PI3K. The dependence of FcγR-mediated phagocytosis on PI3K is well documented (Araki et al., 1996; Cox et al., 1999) and ongoing work in our laboratory has demonstrated that the production of 3,4,5-$PIP_3$ is exquisitely restricted to the forming phagosome. Hence, consumption of 4,5-$PIP_2$ by PI3K must contribute to the dissociation of PLCδ-PH-GFP. Finally, hydrolysis of 4,5-$PIP_2$ by PLC can also result in displacement of PLCδ-PH-GFP from phagosomes. The concomitant appearance of DAG argues in favor of a central role of PLC in the depletion of 4,5-$PIP_2$ from phagosomes (Fig. 6 D).

In summary, we detected an exquisitely localized biphasic change in the concentration of 4,5-$PIP_2$ in the region of the plasmalemma that evolves to become the phagosome. This is accompanied by an equally localized, yet somewhat delayed and longer lasting accumulation of DAG. The latter results, at least in part, from activation of PLC, although a contribution of phospholipase D and phosphatidate phosphohydrolase is also possible (Kusner et al., 1999). These focal changes in lipid metabolism are shown diagrammatically in Fig. 10.

### *Localized Phosphoinositide Metabolism Is Required for Phagocytosis*

We found that phagocytosis was markedly inhibited when 4,5-$PIP_2$ was sequestered by addition of neomycin or by overexpression of PLCδ-PH domain. Similarly, enzymatic degradation of 4,5-$PIP_2$ also resulted in diminution of the phagocytic index (Fig. 7). Together, our findings are consistent with the growing notion that 4,5-$PIP_2$ can act as a second messenger in signal transduction. This phospholipid is a regulator of actin capping, nucleation of de novo F-actin, and anchoring, cross-linking, and severing proteins (Hinchliffe et al., 1998), and actin remodeling is essential to the phagocytic process (Kwiatkowska and Sobota, 1999). Thus we tentatively postulate that local accumulation of 4,5-$PIP_2$ might promote the recruitment of cytoskeletal proteins, stimulating F-actin anchorage and remodeling and contributing to the formation of the phagocytic cup (Fig. 10).

The rapid recruitment of PIPKIα to the nascent phagosome suggests that this enzyme contributes to the early phase of 4,5-$PIP_2$ accumulation. It is noteworthy that Rho, Rac, ADP-ribosylation factor 6 (ARF6), and phospholipase D, all reported activators of PIPKIα, are believed to be necessary for phagocytosis (Chong et al., 1994; Cox et al., 1997; Hackam et al., 1997; Zhang et al., 1998; Honda et al., 1999; Kusner et al., 1999; Tolias et al., 2000). The role of these proteins in the recruitment and possible activation of PIPKIα remains to be defined.

In addition to providing docking sites for cytoskeletal components, 4,5-$PIP_2$ generated at the nascent phagosome may serve to produce a renewable source of substrate for PLC and PI3K during phagocytosis, potentiating the signals generated by these enzymes. We found that inactivation of PLC with pharmacological agents and using dominant-inhibitory forms of PLCγ effectively impaired phagocytosis.

What are the possible modes of action of PLC during phagocytosis? The effects of the enzyme may result from the disappearance of its primary substrate, i.e., 4,5-$PIP_2$, or from the generation of its hydrolysis products (Fig. 10 A). The dynamic cytoskeletal changes necessary for completion of phagocytosis may require cycles of actin polymerization and depolymerization. This in turn may necessitate alternating formation and hydrolysis of 4,5-$PIP_2$, possibly involving PLC, as has been suggested for chemotaxis (Chen et al., 1996a; Wells et al., 1999). The products of 4,5-$PIP_2$ hydrolysis may themselves participate in actin remodeling. By competing with the headgroups of the phosphoinositide, $IP_3$ may directly modulate the interaction of cytoskeletal or other proteins bearing PH or Lys/Arg-rich hydrophobic domains (Bottomley et al., 1998; Martin, 1998). In principle, calcium release from stores or the ensuing store-operated influx could also regulate actin remodeling. However, the latter mechanism is likely to play only a minor role in particle internalization, since there is ample evidence that FcγR-mediated phagocytosis in macrophages proceeds in the absence of cytosolic calcium transients (McNeil et al., 1986; Greenberg et al., 1991).

While the involvement of $IP_3$ in phagocytosis is open to question, DAG is more likely to play a critical role in transducing the response. Accordingly, addition of exogenous DAG or its analogues augments phagocytosis (Karimi et al., 1999), an effect that has been attributed to PKC isoforms. In agreement with this postulate, both PKCα and PKCδ copurify with isolated phagosomal membranes (Allen and Aderem, 1995; Brumell et al., 1999) and some inhibitors of PKC activity have been reported to interfere with phagocytosis (Zheleznyak and Brown, 1992; Karimi et al., 1999). However, discrepant findings abound (Greenberg et al., 1993) and our own unpublished observations also failed to demonstrate an absolute requirement for PKC. The inconsistencies may be attributed to variability in the experimental systems used or to the fact that PKC isoforms sometimes have opposing effects on actin assembly, but it is also possible that C1 domain–containing proteins other than PKC may mediate the effects of DAG in coordinating phagocytosis. There are currently close to 50 proteins with typical C1 domains, including the chimaerin family of Rac GTPase-activating proteins (Caloca et al., 1999) and RasGRP (Lorenzo et al., 2000). Furthermore, a nucleotide exchange factor for Rap1 is also regulated by DAG (Kawasaki et al., 1998). Interestingly, this GTPase is enriched in mammalian phagosomes (Pizon et al., 1994) and its homologue was found to be indispensable for phagocytosis in *Dictyostelium* (Seastone et al., 1999). One or more of these DAG-binding proteins, rather than PKC isoforms, may be the effectors ultimately activated by PLC.

In conclusion, our results reveal the induction of localized and transient changes in 4,5-$PIP_2$ metabolism in the nascent phagosome. These observations suggest that net changes in the focal concentration of the phosphoinositide contribute to remodeling of F-actin in the phagosomal cup (Fig. 10). In addition, one or more products of its metabolism, including DAG and 3,4,5-$PIP_3$, are likely to play essential roles in pseudopod extension and phagosome closure.

This work was supported by the Medical Research Council of Canada, the Arthritis Society of Canada, and the National Sanatorium Association. R.J. Botelho is the recipient of a studentship from Natural Sciences and Engineering Council of Canada. S. Grinstein is an International Scholar of the Howard Hughes Medical Institute and is the current holder of the Pitblado Chair in Cell Biology.

Submitted: 30 May 2000
Revised: 12 September 2000
Accepted: 3 November 2000

### *References*

Allen, L.H., and A. Aderem. 1995. A role for MARCKS, the α isozyme of protein kinase C and myosin I in zymosan phagocytosis by macrophages. *J. Exp. Med*. 182:829–840.

Araki, N., M.T. Johnson, and J.A. Swanson. 1996. A role for phosphoinositide 3-kinase in the completion of macropinocytosis and phagocytosis by macrophages. *J. Cell Biol*. 135:1249–1260.

Azzoni, L., M. Kamoun, T.W. Salcedo, P. Kanakaraj, and B. Perussia. 1992. Stimulation of FcγRIIIA results in phospholipase C-γ 1 tyrosine phosphorylation and $p56^{lck}$ activation. *J. Exp. Med*. 176:1745–1750.

Beron, W., C. Alvarez-Dominguez, L. Mayorga, and P.D. Stahl. 1995. Membrane trafficking along the phagocytic pathway. *Trends Cell Biol*. 5:100–104.

Bottomley, M.J., K. Salim, and G. Panayotou. 1998. Phospholipid-binding protein domains. *Biochim. Biophys. Acta*. 1436:165–183.

Brumell, J.H., J.C. Howard, K. Craig, S. Grinstein, A.D. Schreiber, and M. Tyers. 1999. Expression of the protein kinase C substrate pleckstrin in macrophages: association with phagosomal membranes. *J. Immunol*. 163:3388–3395.

Caloca, M.J., M.L. Garcia-Bermejo, P.M. Blumberg, N.E. Lewin, E. Kremmer, H. Mischak, S. Wang, K. Nacro, B. Bienfait, V.E. Marquez, and M.G. Kazanietz. 1999. β2-chimaerin is a novel target for diacylglycerol: binding properties and changes in subcellular localization mediated by ligand binding to its C1 domain. *Proc. Natl. Acad. Sci. USA*. 96:11854–11859.

Caron, E., and A. Hall. 1998. Identification of two distinct mechanisms of phagocytosis controlled by different Rho GTPases. *Science*. 282:1717–1721.

Chen, P., J.E. Murphy-Ullrich, and A. Wells. 1996a. A role for gelsolin in actuating epidermal growth factor receptor–mediated cell motility. *J. Cell Biol.* 134:689–698.

Chen, P., H. Xie, and A. Wells. 1996b. Mitogenic signaling from the EGF receptor is attenuated by a phospholipase C-γ/protein kinase C feedback mechanism. *Mol. Biol. Cell*. 7:871–881.

Cheng, P.C., M.L. Dykstra, R.N. Mitchell, and S.K. Pierce. 1999. A role for lipid rafts in B cell antigen receptor signaling and antigen targeting. *J. Exp. Med.* 190:1549–1560.

Chong, L.D., A. Traynor-Kaplan, G.M. Bokoch, and M.A. Schwartz. 1994. The small GTP-binding protein Rho regulates a phosphatidylinositol 4-phosphate 5-kinase in mammalian cells. *Cell*. 79:507–513.

Cox, D., P. Chang, Q. Zhang, P.G. Reddy, G.M. Bokoch, and S. Greenberg. 1997. Requirements for both Rac1 and Cdc42 in membrane ruffling and phagocytosis in leukocytes. *J. Exp. Med.* 186:1487–1494.

Cox, D., C.C. Tseng, G. Bjekic, and S. Greenberg. 1999. A requirement for phosphatidylinositol 3-kinase in pseudopod extension. *J. Biol. Chem.* 274: 1240–1247.

Crowley, M.T., P.S. Costello, C.J. Fitzer-Attas, M. Turner, F. Meng, C. Lowell, V.L. Tybulewicz, and A.L. DeFranco. 1997. A critical role for Syk in signal transduction and phagocytosis mediated by Fcγ receptors on macrophages. *J. Exp. Med.* 186:1027–1039.

Czech, M.P. 2000. PIP2 and PIP3: complex roles at the cell surface. *Cell*. 100: 603–606.

Daeron, M. 1997. Fc receptor biology. *Annu. Rev. Immunol.* 15:203–234.

Greenberg, S., J. el Khoury, F. di Virgilio, E.M. Kaplan, and S.C. Silverstein. 1991. $Ca^{2+}$-independent F-actin assembly and disassembly during Fc receptor–mediated phagocytosis in mouse macrophages. *J. Cell Biol.* 113:757–767.

Greenberg, S., P. Chang, and S.C. Silverstein. 1993. Tyrosine phosphorylation is required for Fc receptor–mediated phagocytosis in mouse macrophages. *J. Exp. Med.* 177:529–534.

Greenberg, S., P. Chang, and S.C. Silverstein. 1994. Tyrosine phosphorylation of the γ subunit of Fcγ receptors, p72syk, and paxillin during Fc receptor-mediated phagocytosis in macrophages. *J. Biol. Chem.* 269:3897–3902.

Hackam, D.J., O.D. Rotstein, A. Schreiber, W. Zhang, and S. Grinstein. 1997. Rho is required for the initiation of calcium signaling and phagocytosis by Fcγ receptors in macrophages. *J. Exp. Med.* 186:955–966.

Hinchliffe, K.A., A. Ciruela, and R.F. Irvine. 1998. PIPkins1, their substrates and their products: new functions for old enzymes. *Biochim. Biophys. Acta.* 1436:87–104.

Hishikawa, T., J.Y. Cheung, R.V. Yelamarty, and D.W. Knutson. 1991. Calcium transients during Fc receptor–mediated and nonspecific phagocytosis by murine peritoneal macrophages. *J. Cell Biol.* 115:59–66.

Honda, A., M. Nogami, T. Yokozeki, M. Yamazaki, H. Nakamura, H. Watanabe, K. Kawamoto, K. Nakayama, A.J. Morris, M.A. Frohman, and Y. Kanaho. 1999. Phosphatidylinositol 4-phosphate 5-kinase α is a downstream effector of the small G protein ARF6 in membrane ruffle formation. *Cell*. 99:521–532.

Karimi, K., T.R. Gemmill, and M.R. Lennartz. 1999. Protein kinase C and a calcium-independent phospholipase are required for IgG-mediated phagocytosis by Mono-Mac-6 cells. *J. Leukoc. Biol.* 65:854–862.

Kavran, J.M., D.E. Klein, A. Lee, M. Falasca, S.J. Isakoff, E.Y. Skolnik, and M.A. Lemmon. 1998. Specificity and promiscuity in phosphoinositide binding by pleckstrin homology domains. *J. Biol. Chem.* 273:30497–30508.

Kawasaki, H., G.M. Springett, S. Toki, J.J. Canales, P. Harlan, J.P. Blumenstiel, E.J. Chen, I.A. Bany, N. Mochizuki, A. Ashbacher, et al. 1998. A Rap guanine nucleotide exchange factor enriched highly in the basal ganglia. *Proc. Natl. Acad. Sci. USA*. 95:13278–13283.

Kiefer, F., J. Brumell, N. Al-Alawi, S. Latour, A. Cheng, A. Veillette, S. Grinstein, and T. Pawson. 1998. The Syk protein tyrosine kinase is essential for Fcγ receptor signaling in macrophages and neutrophils. *Mol. Cell. Biol*. 18: 4209–4220.

Kontos, C.D., T.P. Stauffer, W.P. Yang, J.D. York, L. Huang, M.A. Blanar, T. Meyer, and K.G. Peters. 1998. Tyrosine 1101 of Tie2 is the major site of association of p85 and is required for activation of phosphatidylinositol 3-kinase and Akt. *Mol. Cell. Biol*. 18:4131–4140.

Kusner, D.J., C.F. Hall, and S. Jackson. 1999. Fcγ receptor-mediated activation of phospholipase D regulates macrophage phagocytosis of IgG-opsonized particles. *J. Immunol*. 162:2266–2274.

Kwiatkowska, K., and A. Sobota. 1999. Signaling pathways in phagocytosis. *Bioessays*. 21:422–431.

Lemmon, M.A., K.M. Ferguson, R. O'Brien, P.B. Sigler, and J. Schlessinger. 1995. Specific and high-affinity binding of inositol phosphates to an isolated pleckstrin homology domain. *Proc. Natl. Acad. Sci. USA*. 92:10472–10476.

Lew, D.P., T. Andersson, J. Hed, F. Di Virgilio, T. Pozzan, and O. Stendahl. 1985. $Ca^{2+}$-dependent and $Ca^{2+}$-independent phagocytosis in human neutrophils. *Nature*. 315:509–511.

Liao, F., H.S. Shin, and S.G. Rhee. 1992. Tyrosine phosphorylation of phospholipase C-γ1 induced by cross-linking of the high-affinity or low-affinity Fc receptor for IgG in U937 cells. *Proc. Natl. Acad. Sci. USA*. 89:3659–3663.

Lorenzo, P.S., M. Beheshti, G.R. Pettit, J.C. Stone, and P.M. Blumberg. 2000. The guanine nucleotide exchange factor RasGRP is a high-affinity target for diacylglycerol and phorbol esters. *Mol. Pharmacol*. 57:840–846.

Martin, T.F. 1998. Phosphoinositide lipids as signaling molecules: common themes for signal transduction, cytoskeletal regulation, and membrane trafficking. *Annu. Rev. Cell Dev. Biol.* 14:231–264.

Massol, P., P. Montcourrier, J.C. Guillemot, and P. Chavrier. 1998. Fc receptor-mediated phagocytosis requires CDC42 and Rac1. *EMBO (Eur. Mol. Biol. Organ.) J*. 17:6219–6229.

McNeil, P.L., J.A. Swanson, S.D. Wright, S.C. Silverstein, and D.L. Taylor. 1986. Fc receptor-mediated phagocytosis occurs in macrophages without an increase in average $[Ca^{++}]_i$. *J. Cell Biol*. 102:1586–1592.

Mochizuki, Y., and T. Takenawa. 1999. Novel inositol polyphosphate 5-phosphatase localizes at membrane ruffles. *J. Biol. Chem*. 274:36790–36795.

Ninomiya, N., K. Hazeki, Y. Fukui, T. Seya, T. Okada, O. Hazeki, and M. Ui. 1994. Involvement of phosphatidylinositol 3-kinase in Fcγ receptor signaling. *J. Biol. Chem*. 269:22732–22737.

Oancea, E., and T. Meyer. 1998. Protein kinase C as a molecular machine for decoding calcium and diacylglycerol signals. *Cell*. 95:307–318.

Oancea, E., M.N. Teruel, A.F. Quest, and T. Meyer. 1998. Green fluorescent protein (GFP)-tagged cysteine-rich domains from protein kinase C as fluorescent indicators for diacylglycerol signaling in living cells. *J. Cell Biol*. 140:485–498.

Pizon, V., M. Desjardins, C. Bucci, R.G. Parton, and M. Zerial. 1994. Association of Rap1a and Rap1b proteins with late endocytic/phagocytic compartments and Rap2a with the Golgi complex. *J. Cell Sci*. 107:1661–1670.

Raucher, D., T. Stauffer, W. Chen, K. Shen, S. Guo, J.D. York, M.P. Sheetz, and T. Meyer. 2000. Phosphatidylinositol 4,5-bisphosphate functions as a second messenger that regulates cytoskeleton-plasma membrane adhesion. *Cell*. 100:221–228.

Ren, X.D., and M.A. Schwartz. 1998. Regulation of inositol lipid kinases by Rho and Rac. *Curr. Opin. Genet. Dev*. 8:63–67.

Rhee, S.G., and Y.S. Bae. 1997. Regulation of phosphoinositide-specific phospholipase C isozymes. *J. Biol. Chem*. 272:15045–15048.

Seastone, D.J., L. Zhang, G. Buczynski, P. Rebstein, G. Weeks, G. Spiegelman, and J. Cardelli. 1999. The small $M_r$ Ras-like GTPase Rap1 and the phospholipase C pathway act to regulate phagocytosis in *Dictyostelium discoideum*. *Mol. Biol. Cell*. 10:393–406.

Sheterline, P., J.E. Rickard, and R.C. Richards. 1984. Fc receptor-directed phagocytic stimuli induce transient actin assembly at an early stage of phagocytosis in neutrophil leukocytes. *Eur. J. Cell Biol*. 34:80–87.

Shibasaki, Y., H. Ishihara, N. Kizuki, T. Asano, Y. Oka, and Y. Yazaki. 1997. Massive actin polymerization induced by phosphatidylinositol-4-phosphate 5-kinase *in vivo*. *J. Biol. Chem*. 272:7578–7581.

Stauffer, T.P., and T. Meyer. 1997. Compartmentalized IgE receptor–mediated signal transduction in living cells. *J. Cell Biol*. 139:1447–1454.

Stauffer, T.P., S. Ahn, and T. Meyer. 1998. Receptor-induced transient reduction in plasma membrane $PtdIns(4,5)P_2$ concentration monitored in living cells. *Curr. Biol*. 8:343–346.

Teruel, M.N., T.A. Blanpied, K. Shen, G.J. Augustine, and T. Meyer. 1999. A versatile microporation technique for the transfection of cultured CNS neurons. *J. Neurosci. Methods*. 93:37–48.

Tolias, K.F., L.C. Cantley, and C.L. Carpenter. 1995. Rho family GTPases bind

to phosphoinositide kinases. *J. Biol. Chem*. 270:17656–17659.
Tolias, K.F., J.H. Hartwig, H. Ishihara, Y. Shibasaki, L.C. Cantley, and C.L. Carpenter. 2000. Type Iα phosphatidylinositol-4-phosphate 5-kinase mediates Rac-dependent actin assembly. *Curr. Biol*. 10:153–156.
Varnai, P., and T. Balla. 1998. Visualization of phosphoinositides that bind pleckstrin homology domains: calcium- and agonist-induced dynamic changes and relationship to *myo*-[$^3$H]inositol–labeled phosphoinositide pools. *J. Cell Biol*. 143:501–510.
Varnai, P., K.I. Rother, and T. Balla. 1999. Phosphatidylinositol 3-kinase-dependent membrane association of the Bruton's tyrosine kinase pleckstrin homology domain visualized in single living cells. *J. Biol. Chem*. 274:10983–10989.
Wells, A., M.F. Ware, F.D. Allen, and D.A. Lauffenburger. 1999. Shaping up for shipping out: PLCγ signaling of morphology changes in EGF-stimulated fibroblast migration. *Cell. Motil. Cytoskeleton*. 44:227–233.
Zhang, Q., D. Cox, C.C. Tseng, J.G. Donaldson, and S. Greenberg. 1998. A requirement for ARF6 in Fcγ receptor-mediated phagocytosis in macrophages. *J. Biol. Chem*. 273:19977–19981.
Zhang, X., J.C. Loijens, I.V. Boronenkov, G.J. Parker, F.A. Norris, J. Chen, O. Thum, G.D. Prestwich, P.W. Majerus, and R.A. Anderson. 1997. Phosphatidylinositol-4-phosphate 5-kinase isozymes catalyze the synthesis of 3-phosphate-containing phosphatidylinositol signaling molecules. *J. Biol. Chem*. 272:17756–17761.
Zheleznyak, A., and E.J. Brown. 1992. Immunoglobulin-mediated phagocytosis by human monocytes requires protein kinase C activation. Evidence for protein kinase C translocation to phagosomes. *J. Biol. Chem*. 267:12042–12048.